Matrix Biology xxx (2014) xxx–xxx

Contents lists available at ScienceDirect

Matrix Biology

journal homepage: www.elsevier.com/locate/matbio

Absence of substance P and the sympathetic nervous system impact on bone structure and chondrocyte differentiation in an adult model of endochondral ossification

Q1 Tanja Niedermair [a,b], Volker Kuhn [c], Doraneh Gard Fatameh [a,b], Richard Stange [d], Britta Wieskötter [d], Johannes Beckmann [a], Philipp Salmen [c], Hans-Robert Springorum [a], Rainer H. Straub [e], Andreas Zimmer [f], Joachim Grifka [a], Susanne Grässel [a,b,*]

[a] Department of Orthopaedic Surgery, University of Regensburg, Germany
[b] Department of Orthopaedic Surgery, Experimental Orthopaedics, Centre for Medical Biotechnology, University of Regensburg, Germany
[c] Department of Trauma Surgery, Medical University Innsbruck, Austria
[d] Department of Trauma, Hand and Reconstructive Surgery, University Hospital, Münster, Germany
[e] Laboratory of Experimental Rheumatology and Neuroendocrine Immunology, Department of Internal Medicine I, University of Regensburg, Germany
[f] Institute for Molecular Psychiatry, University of Bonn, Germany

ARTICLE INFO

Article history:
Received 24 January 2014
Received in revised form 27 June 2014
Accepted 29 June 2014
Available online xxxx

Keywords:
Substance P
Sympathetic nerve fibers
Fracture callus
Bone structure
Bone formation
Bone resorption
Biomechanics
Endochondral ossification

ABSTRACT

Q2 *Objective:* Sensory and sympathetic nerve fibers (SNF) innervate bone and epiphyseal growth plate. The role of neuronal signals for proper endochondral ossification during skeletal growth is mostly unknown. Here, we investigated the impact of the absence of sensory neurotransmitter substance P (SP) and the removal of SNF on callus differentiation, a model for endochondral ossification in adult animals, and on bone formation.
Methods: In order to generate callus, tibia fractures were set in the left hind leg of wild type (WT), tachykinin 1-deficient (Tac1 −/−) mice (no SP) and animals without SNF. Locomotion was tested in healthy animals and touch sensibility was determined early after fracture. Callus tissue was prepared for immunofluorescence staining for SP, neurokinin1-receptor (NK1R), tyrosine-hydroxylase (TH) and adrenergic receptors α1, α2 and β2. At the fracture site, osteoclasts were stained for TRAP, osteoblasts were stained for RUNX2, and histomorphometric analysis of callus tissue composition was performed. Primary murine bone marrow derived macrophages (BMM), osteoclasts, and osteoblasts were tested for differentiation, activity, proliferation and apoptosis in vitro. Femoral fractures were set in the left hind leg of all the three groups for mechanical testing and μCT-analysis.
Results: Callus cells stained positive for SP, NK1R, α1d- and α2b adrenoceptors and remained β2-adrenoceptor and TH-negative. Absence of SP and SNF did not change the general locomotion but reduces touch sensitivity after fracture. In mice without SNF, we detected more mesenchymal callus tissue and less cartilaginous tissue 5 days after fracture. At day 13 past fracture, we observed a decrease of the area covered by hypertrophic chondrocytes in Tac1 −/− mice and mice without SNF, a lower number of osteoblasts in Tac1 −/− mice and an increase of osteoclasts in mineralized callus tissue in mice without SNF. Apoptosis rate and activity of BMM, osteoclasts and osteoblasts isolated from Tac1 −/− and sympathectomized mice were partly altered in vitro. Mechanical testing of fractured- and contralateral legs 21 days after fracture, revealed an overall reduced mechanical bone quality in Tac1 −/− mice and mice without SNF. μCT-analysis revealed clear structural alteration in contralateral and fractured legs proximal of the fracture site with respect to trabecular parameters, bone mass and connectivity density. Notably, structural parameters are altered in fractured legs when related to unfractured legs in WT but not in mice without SP and SNF.
Conclusion: The absence of SP and SNF reduces pain sensitivity and mechanical stability of the bone in general. The micro-architecture of the bone is profoundly impaired in the absence of intact SNF with a less drastic effect in SP-deficient mice. Both sympathetic and sensory neurotransmitters are indispensable for proper callus differentiation. Importantly, the absence of SP reduces bone formation rate whereas the absence of SNF induces bone resorption rate. Notably, fracture chondrocytes produce SP and its receptor NK1 and are positive for α-adrenoceptors indicating an endogenous callus signaling loop. We propose that sensory and sympathetic

* Corresponding author at: Department of Orthopaedics, University of Regensburg, ZMB/BioPark 1 Josef-Engert-Str. 9, 93053 Regensburg, Germany. Tel.: +49 941 943 5065; fax: +49 941 943 5066.
E-mail address: susanne.graessel@klinik.uni-regensburg.de (S. Grässel).

http://dx.doi.org/10.1016/j.matbio.2014.06.007

neurotransmitters have crucial trophic effects which are essential for proper bone formation in addition to their classical neurological actions.

1. Introduction

The process of callus differentiation during fracture healing is believed to reinitiate molecular pathways at the fracture site that take place during embryonic skeletal development and closely resemble endochondral ossification (Einhorn, 1998). Thus, endochondral ossification in the process of callus maturation is an ideal system for addressing fundamental questions underlying skeletal tissue regeneration, remineralization and remodeling in adults. The extent of fracture stabilization affects callus size and formation. Under rigid, stable fixation regimen, bone regenerates with no or only minor callus formation (Claes and Heigele, 1999);(Claes et al., 1995). When applying more flexible fixation regimens, bone healing occurs in consecutive stages which involve intense callus formation. Firstly, an acute inflammatory response and recruitment of mesenchymal stem cells (mesenchymal callus) occur in order to subsequently generate a primary cartilaginous callus populated mostly with chondrocytes (soft callus). Later, this cartilaginous callus undergoes revascularization and calcification (calcified hard callus) and is finally remodeled to fully restore a normal bony structure and architecture (Marsell and Einhorn, 2011).

Bone and periosteum are innervated by sympathetic and sensory nerve fibers suggesting that the peripheral nervous system is involved in bone metabolism (Lerner, 2002; Jones et al., 2004). These nerve fibers contain, among others, the catecholaminergic key enzyme tyrosine hydroxylase (TH) and the sensory neuropeptide substance P (SP) (Bjurholm et al., 1988a,1988b; Garcia-Castellano et al., 2000). Experimental studies provided accumulating evidence that peripheral nerve fibers also innervate the fracture site and influence repair mechanism after trauma (Hukkanen et al., 1993). At early time points after fracture, peripheral nerve fibers grow into callus prior to vascularization indicating that a restored nerve supply could be essential for normal fracture healing (Li et al., 2001). Aro et al., showed that in denervated limbs fracture callus size was reduced at a later stage (Aro, 1985). By contrast, there are some studies that demonstrated larger callus formation after nerve resection (Nordsletten et al., 1994; Madsen et al., 1998). These studies are based on limb denervation of ipsilateral peripheral nerve fibers, thereby, changing total neuronal influence at the fracture site which makes it difficult to determine contribution of individual neuronal pathways to specific changes in callus formation.

Substance P belongs to the tachykinin neuropeptide family and is the major neuropeptide synthesized from the pre-protachykinin-A (*Tac1*) gene. Tachykinins mediate their biological effects via three different neurokinin (NK1, 2, 3) receptors. Among these, SP has the highest affinity to NK1 receptor (NK1R) (Harrison and Geppetti, 2001; Severini et al., 2002). SP plays a role in pain transmission; tibial fractures cause an early and strong induction of sensory nerve regeneration and growth into the site of injury (sensory sprouting) (Hukkanen et al., 1995). The presence of NK1 receptors was demonstrated on bone cells (Goto et al., 1998), and studies on SP and its putative role in bone tissue showed that it can stimulate osteogenesis (Shih and Bernard, 1997) and late stage osteoblastic bone formation (Mori et al., 1999; Goto et al., 2007). SP is involved in regulating bone remodeling through controlling osteoclast differentiation (Wang et al., 2009) and affecting proliferation in a variety of cell types such as osteoblasts, bone marrow mesenchymal stem cells, synovial fibroblastic cells, and T- or B-lymphocytes (Nilsson et al., 1985; Liu et al., 2007). Recently we demonstrated that murine costal chondrocytes express SP and NK1 receptors and that SP stimulation dose-dependently increases chondrocyte proliferation rate and induces formation of focal adhesion contacts (Opolka et al., 2012).

Sympathetic nerve fibers (SNF) have been identified in bone marrow, in periosteum, and in bone-adherent ligaments (Bjurholm et al., 1990; Imai and Matsusue, 2002) hereby, affecting bone mass (Elefteriou et al., 2005; Yirmiya et al., 2006). Catecholamines mediate their actions by binding to adrenergic receptors, a class of G protein-coupled receptors with different subtypes (α_1, α_2, β_1, β_2, β_3). In the musculoskeletal system, both, α- and β-adrenergic subtypes were found on osteoblasts (Huang et al., 2009), osteoclasts (Aitken et al., 2009) and chondrocytes (Aitken et al., 2009; Huang et al., 2009; Opolka et al., 2012). These findings indicate that skeletal growth or activity of bone tissue might be regulated by SNF. Indeed, the group of Karsenty has demonstrated that the sympathetic nervous system (SNS) is a master player of bone homeostasis (Amling et al., 2000; Ducy et al., 2000; Takeda et al., 2002). β-adrenergic receptors on osteoblasts regulate proliferation, and β-adrenergic agonists decrease bone mass while β-adrenergic antagonists increase bone mass (Elefteriou et al., 2005). This observation is in line with a stimulatory effect on osteoclastogenesis via β-adrenergic signaling (Kondo et al., 2013). Despite some controversial studies, it also seems that β-blockers in humans reduce the risk of bone fracture and osteoporosis as recently summarized in a metaanalysis (Wiens et al., 2006).

Abundance of sympathetic and sensory nerve fibers near the bone and the presence of neurotransmitter receptors on bone cells imply crucial functions in bone metabolism, however, the direct effects of these nerve fibers and their specific neurotransmitters on bone formation and skeletal growth are still incompletely understood. Therefore, the aim of this study was to investigate the role of substance P and catecholaminergic SNF in callus differentiation as a model for endochondral ossification in adults. As readout we analyzed callus tissue composition and mechanical and structural properties of the bone.

2. Results

2.1. SP and NK1R expression in fracture callus

WT callus tissue was stained for SP and its receptor NK1 during the time course of callus differentiation by immunofluorescence (Fig. 1A). At day 5 after fracture, when chondrogenic differentiation starts, a substantial number of mesenchymal and chondrocyte-like cells stained positive for NK1R and some cells double-stained for SP. At day 9 after fracture, when most of the callus matrix has adopted a cartilaginous phenotype (soft callus), nearly all of the callus chondrocytes were SP- and NK1R-positive (data not shown). At 13 days after fracture, when remodeling of the callus progressed toward tissue mineralization and the bony, hard callus was about to be formed, number of SP-positive callus cells appeared to be reduced compared to day 9 but NK1R staining seems to be unaltered in hypertrophic chondrocytes. SP- and NK1R staining pattern in sympathectomized mice was similar to WT (Supplementary Fig. 1A).

2.2. Sympathetic innervation of the fracture site and adrenergic receptor distribution

To examine sympathetic innervation and/or catecholamine producing cells during callus maturation, we stained WT callus sections for TH (Fig. 1B). At 5 days after fracture, with the appearance of chondrocyte-like cells, TH-positive nerve fibers became displaced toward the callus periphery. Notably, the cartilaginous matrix was not innervated by TH-positive nerve fibers. After 9 days, TH-positive nerve fibers appeared in and near the periosteum (data not shown), where they were still detectable 13 days after fracture (Fig. 1B; white arrowheads).

Please cite this article as: Niedermair, T., et al., Absence of substance P and the sympathetic nervous system impact on bone structure and chondrocyte differentiation in an adult mod..., Matrix Biol. (2014), http://dx.doi.org/10.1016/j.matbio.2014.06.007

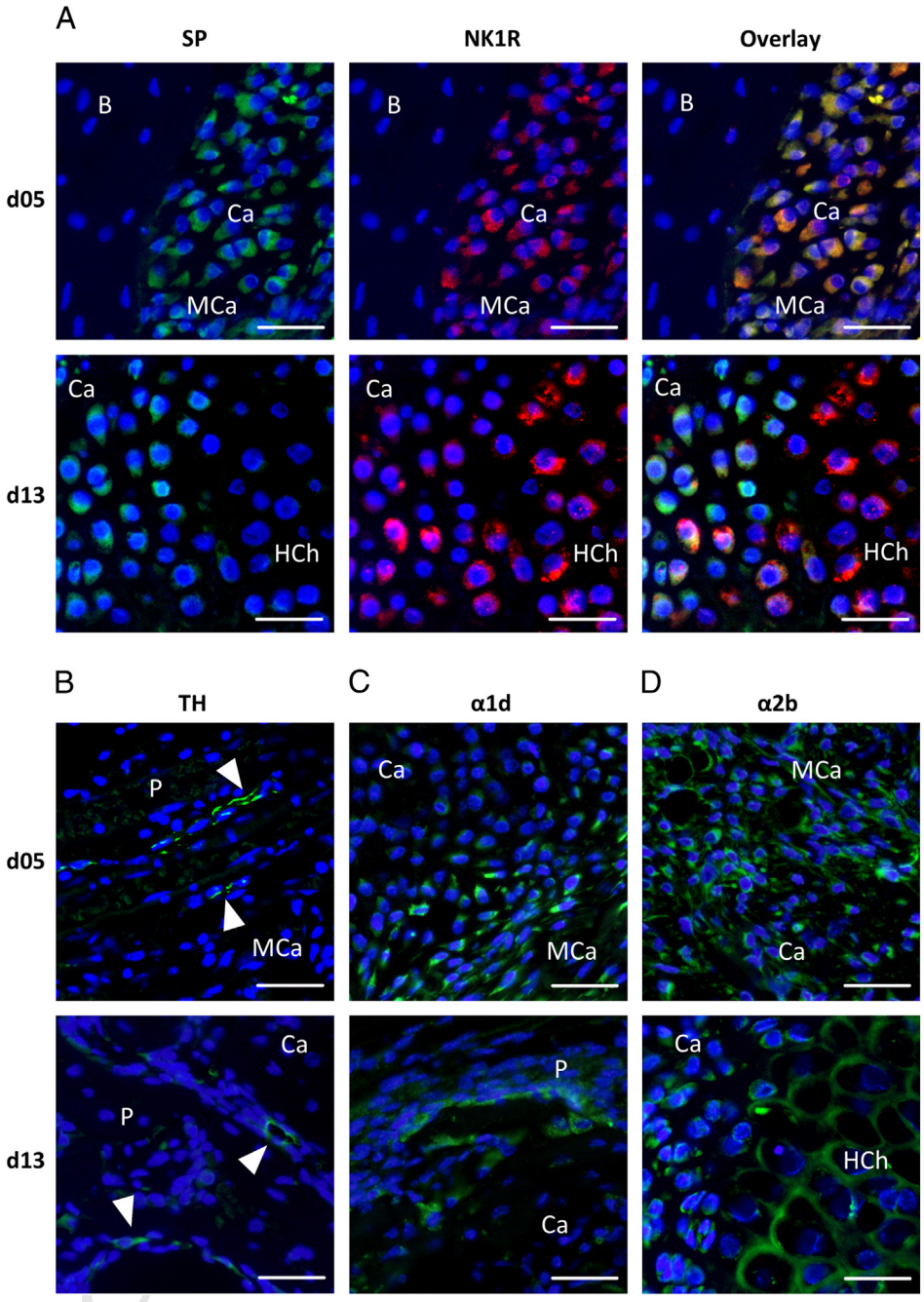

Fig. 1. Distribution of SP, NK1R, TH, α1d and α2b adrenergic receptors at the fracture site. (A) Fluorescence staining of SP- and NK1R-positive cells in fracture callus of WT control mice representative at 5 and 13 days after fracture. SP staining is shown in green (left panel) and NK1R staining is shown in red (middle panel), the overlay of SP and NK1R is visible in yellow (right panel). Scale bar = 50 μm. (B) Fluorescence staining of TH-positive nerve fibers (green) in fracture callus of WT control mice at 5 and 13 days after fracture. White arrowheads mark TH expressing nerve fibers. Scale bar = 50 μm. (C) Fluorescence staining of α1d adrenergic receptor in fracture callus of WT control mice at 5 and 13 days past fracture. Scale bar = 50 μm. (D) Fluorescence staining of α2b adrenergic receptor in fracture callus of WT control mice 5 and 13 days past fracture. Scale bar = 50 μm. Nuclei were stained with DAPI. B = bone, Ca = cartilaginous callus tissue, MCa = mesenchymal callus tissue, HCh = hypertrophic chondrocytes, P = periosteum, M = muscle. (For interpretation of the references to color in this figure legend, the reader is referred to the web version of this article.)

We were unable to locate TH-positive cells within the callus. We observed TH-positive stained nerve fibers in the periosteum of fracture calli of Tac1 −/− mice with no obvious difference in distribution to WT (Supplementary Fig. 1B).

Staining fracture callus tissue for adrenergic receptors demonstrated that mesenchymal callus cells and periosteum stained positive for α1d adrenergic receptor 5 days after fracture whereas only few chondrocyte-like cells were α1d-positive (Fig. 1C). We did not detect α1d-positive cells in cartilaginous and calcified callus tissue (Fig. 1C). Strong α2b adrenergic receptor staining was detected on mesenchymal and chondrocytic callus cells 5 days (Fig. 1D) and 9 days (data not shown) after fracture. At day 13, hypertrophic chondrocytes and also callus cells in calcified callus tissue were intensely stained for α2b-adrenergic receptors (Fig. 1D). We were unable to detect β2-adrenergic receptors in callus cells but in peripheral callus tissue as periosteum (data not shown).

2.3. Morphometrical analysis of callus tissue composition

Morphometrical examination of different callus tissue types (Fig. 2C) at day 5 (Fig. 2A), day 9 (data not shown) and day 13 (Fig. 2B) after

Please cite this article as: Niedermair, T., et al., Absence of substance P and the sympathetic nervous system impact on bone structure and chondrocyte differentiation in an adult mod..., Matrix Biol. (2014), http://dx.doi.org/10.1016/j.matbio.2014.06.007

fracture, revealed that sympathectomized mice had a significantly higher fraction of mesenchymal callus tissue and a lower fraction of cartilaginous callus tissue at day 5 after fracture compared to controls (Supplementary Fig. 2A, C, E). These differences disappeared at days 9 and 13. Tissue composition of fracture callus of Tac1 −/− mice was indistinguishable compared to WT or sympathectomized mice at all time points investigated. However, the proportion of the area covered by collagen X-stained hypertrophic chondrocytes in relation to the total area of cartilaginous soft callus tissue was smaller in fracture callus of Tac1 −/− and sympathectomized mice compared to WT mice at day 13 after fracture (Fig. 2D and Supplementary Fig. 2B, D, F).

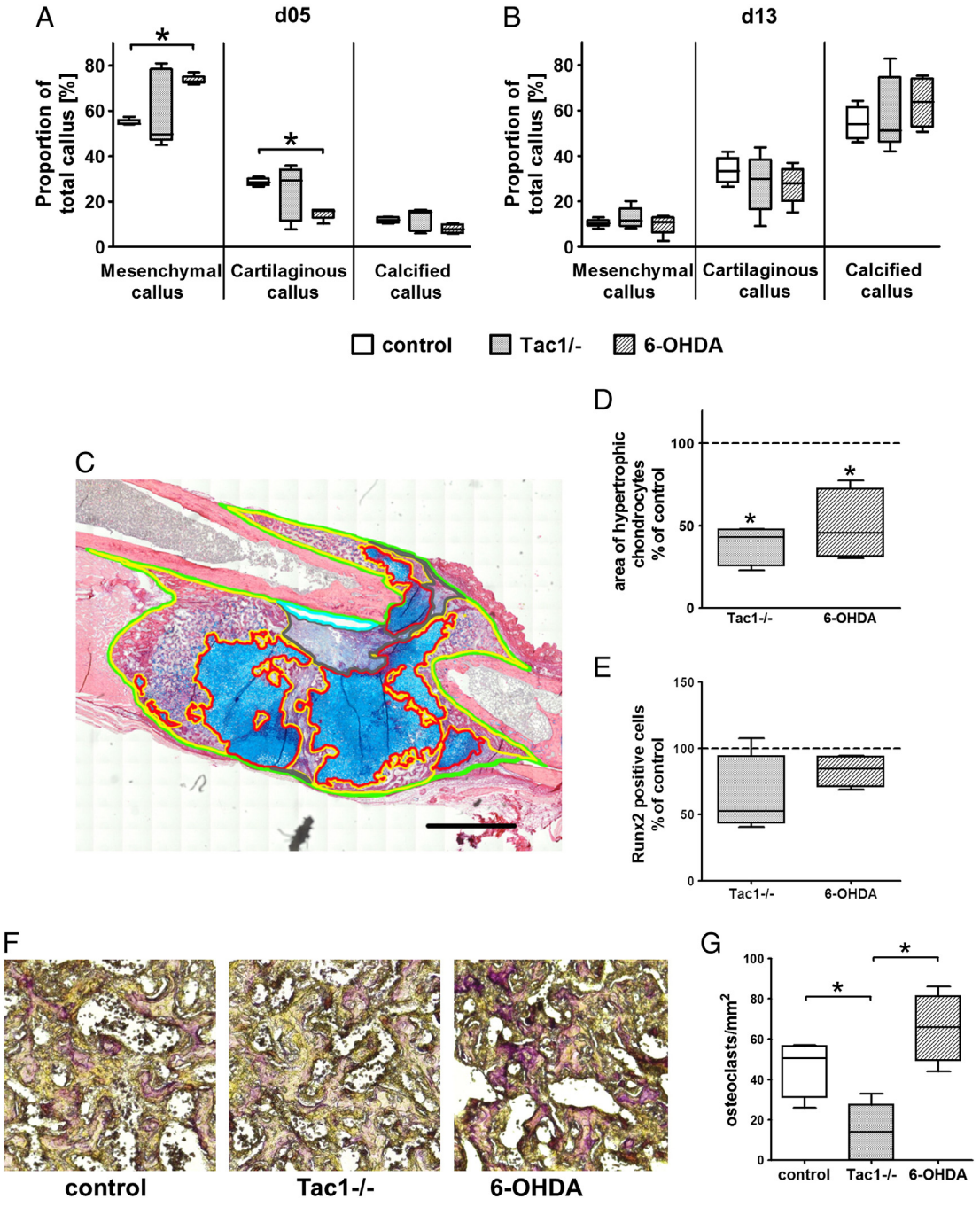

Fig. 2. Histomorphometric analysis of mesenchymal, cartilaginous and calcified callus tissue and osteoblast and osteoclast numbers in calcified callus regions. Proportion of respective callus tissues was determined as percentage of total fracture callus tissue of WT controls (n = 4), Tac1 −/− (n = 5) and sympathectomized mice (n = 4) (6-Hydroxydopamine/6-OHDA application to destroy sympathetic nerve fibers). Graphs show alteration in tissue composition during time course of fracture healing from day 5 (A) and day 13 (B) after setting fractures. (C) Representative overview image of a callus from WT control mice at day 13 after fracture, stained with Alcian blue and Sirius red. Colored lines circle ROI according to tissue type. Green line: total callus (100%); red line: cartilaginous callus; yellow line: calcified callus; blue line: non-stained areas (loss of tissue during to staining procedure), gray line: mesenchymal callus (determined by calculation). Scale bar = 1 mm. Relative changes of the proportion of hypertrophic chondrocyte area in the cartilaginous callus were determined at day 13 (D) after fracture setting. WT control mice (n = 4) were set as 100%, Tac1 −/− (n = 5) and sympathectomized mice (n = 4) were calibrated to these controls. Comparison of number of RUNX2-positive stained osteoblasts in fracture callus of WT (n = 4), Tac1 −/− (n = 4) and sympathectomized (n = 4) mice (E), calculated in percentage (WT control values were set as 100%). Comparison of number of TRAP-stained osteoclasts/mm^2 in calcified callus area of WT controls (n = 4), Tac1 −/− (n = 5) and sympathectomized mice (n = 4). (F) Detailed representative images of osteoclasts in calcified callus tissue (TRAP stained) (100× magnification); of WT control, Tac1 −/− and sympathectomized mice. (G) Histomorphometrical analysis of osteoclast number per mm^2. Data are shown as mean ± SD; * $p < 0.05$.

Please cite this article as: Niedermair, T., et al., Absence of substance P and the sympathetic nervous system impact on bone structure and chondrocyte differentiation in an adult mod..., Matrix Biol. (2014), http://dx.doi.org/10.1016/j.matbio.2014.06.007

2.4. Number of osteoclasts and osteoblasts at the fracture site

In order to analyze whether the absence of SP or SNF influences osteoclast differentiation, osteoclasts in mineralized callus regions were visualized by TRAP staining 13 days past fracture and number of TRAP-positive osteoclasts/mm^2 in calcified callus tissue was determined (Fig. 2F). In fracture callus of control animals, number of TRAP-positive osteoclasts amounted to 46 ± 14 osteoclasts/mm^2. In two fracture callus of Tac1 −/− animals we did not detect any TRAP stained osteoclasts, however the number of TRAP-positive osteoclasts (23 ± 10/mm^2) in three out of five Tac1 −/− fracture callus is significantly lower compared to control and sympathectomized mice. Fracture callus of sympathectomized mice stained intensely TRAP-positive. We counted an average number of 66 ± 17 TRAP-positive osteoclasts/mm^2 which surmounts the number of osteoclasts in fracture callus of Tac1 −/− mice (Fig. 2G).

Osteoblast distribution in the fracture callus was visualized by RUNX2 staining in nuclei 13 days past fracture. 10 pictures of different callus areas (mesenchymal, soft and hard callus tissue) were photographed, the number of RUNX2-positive cells was counted and the values of WT were set as 100%. In three out of four Tac1 −/− fracture callus, the number of RUNX2-positive cells was reduced to about 50% compared to WT whereas in one Tac1 −/− fracture callus a higher osteoblast number (107%) was counted. The numbers of RUNX2-positive osteoblasts in fracture callus of sympathectomized mice and WT are not different (Fig. 2E).

2.5. Osteoclasts differentiated from bone marrow macrophages (BMM) in vitro

Bone marrow macrophages were differentiated into osteoclasts for 5 days in the presence of M-CSF and RANKL. TRAP staining was used to identify differentiated multinucleated osteoclasts. Apoptosis rate is not statistically significantly changed but there is a trend to a higher apoptosis rate of osteoclasts from Tac1 −/− mice whereas the apoptosis rate of osteoclasts from sympathectomized mice is significantly lower compared to Tac1 −/− mice (Fig. 2A). The in vitro capability of BMM from Tac1 −/− and sympathectomized mice to differentiate into osteoclasts is not altered compared to WT (Fig. 3B). Activity of cathepsin K (an enzymatic marker for osteoclasts) was not significantly changed but tends to be higher in osteoclasts from Tac1 −/− and sympathectomized mice compared to WT cells (Fig. 3C).

2.6. Primary osteoblast cultures

Osteoblasts, migrated out from bone chips, were cultured in osteogenic medium for 7 days to analyze apoptosis, proliferation rate and alkaline phosphatase (ALP) activity (Fig. 3D–F). Apoptosis rate of osteoblasts from Tac1 −/− mice was higher compared to osteoblasts of the sympathectomized mice. Apoptosis rate is not altered in osteoblasts from Tac1 −/− and sympathectomized mice when compared to WT (Fig. 3D). Proliferation rate of osteoblasts from Tac1 −/− mice was higher compared to WT although not statistically significant. Proliferation rate is not changed in osteoblasts of sympathectomized mice compared to WT controls (Fig. 3E). Osteoblast metabolic activity was analyzed by measuring the activity of ALP. We determined a significant higher ALP enzyme activity in osteoblasts from sympathectomized mice compared to osteoblasts from Tac1 −/− mice and by tendency a higher ALP activity when compared to WT. ALP activity in osteoblasts from Tac1 −/− mice had high standard deviations which prevented the determination of statistically significant changes compared to WT mice (Fig. 3F).

2.7. Biomechanical evaluation after fracture

In stabilized femoral fractures and contralateral non-fractured femora, mechanical testing was performed at 3 weeks after fracturing. The contralateral non-fractured femora of Tac1 −/− and sympathectomized mice had inferior mechanical properties as resistance to torque (Fig. 4A) and mechanical stiffness (Fig. 4C) when compared with those of WT animals. Contralateral non-fractured femora of WT and sympathectomized mice have a lower angle of failure compared to Tac1 −/− (Fig. 4B) which indicates lower resistance to mechanical strain.

In fractured femora of Tac1 −/− and sympathectomized mice, resistance to torsional failure load was significantly reduced when compared

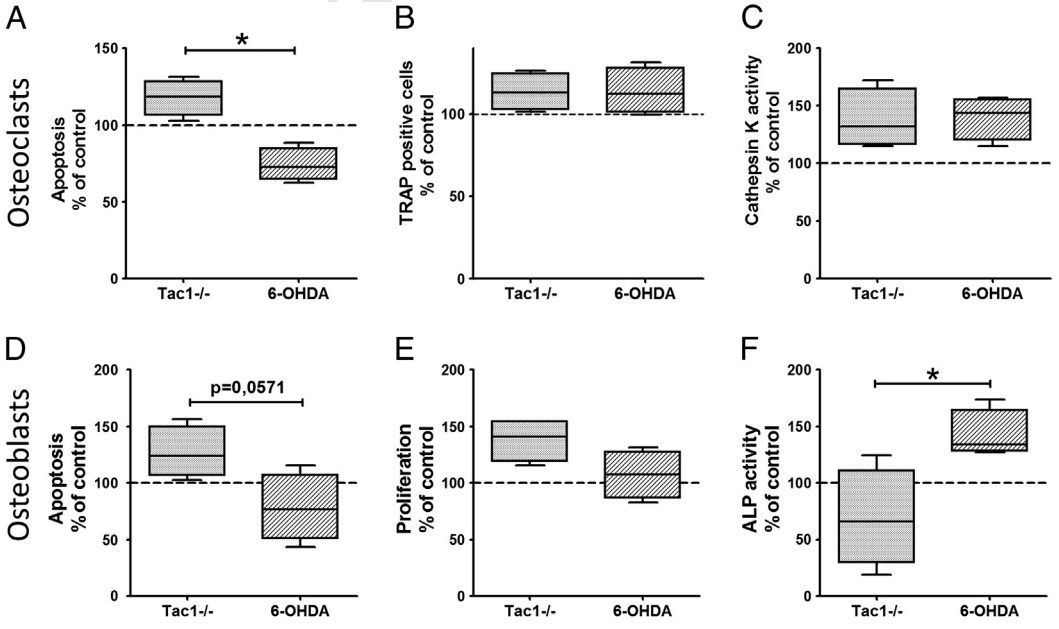

Fig. 3. Apoptosis rate, proliferation rate, differentiation capacity and activity of primary BMM, osteoclasts and osteoblasts. Comparison of apoptosis rate (A), number of TRAP positive cells with ≥3 nuclei (B) and cathepsin K enzyme activity (C) of osteoclasts from WT (n = 4), Tac1 −/− (n = 4) and sympathectomized (n = 4) (6-OHDA application) mice after 5 days differentiation from BMM with M-CSF and RANKL, calculated in percent (WT control values were set as 100%). Comparison of apoptosis rate (D), proliferation rate (E) and alkaline phosphatase (ALP) activity (F) of osteoblasts from WT (n = 4), Tac1 −/− (n = 4) and sympathectomized (n = 4) mice after 7 days of culture in osteogenic medium, calculated in percent (WT control values were set as 100%). Data are shown as mean ± SD; * $p < 0.05$.

Please cite this article as: Niedermair, T., et al., Absence of substance P and the sympathetic nervous system impact on bone structure and chondrocyte differentiation in an adult mod..., Matrix Biol. (2014), http://dx.doi.org/10.1016/j.matbio.2014.06.007

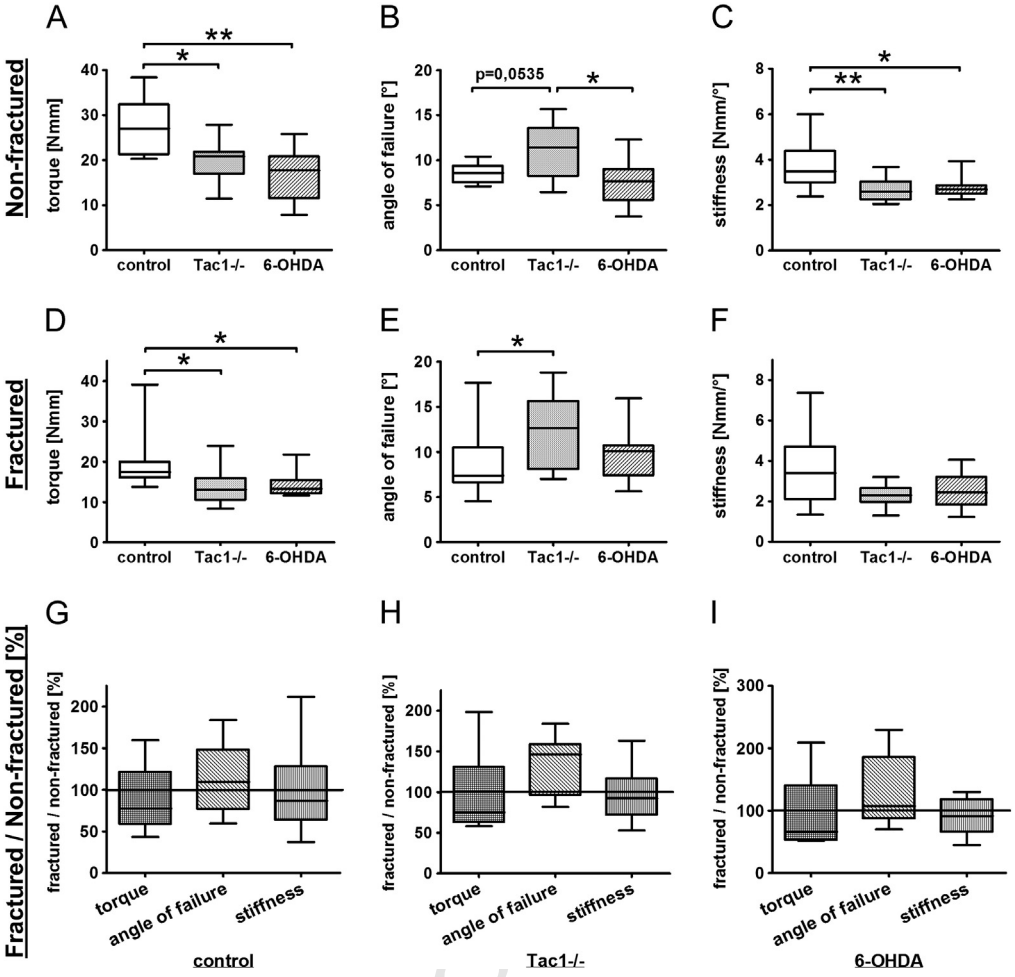

Fig. 4. Determination of mechanical properties of contralateral non-fractured and fractured femora. Comparison of resistance to torque (A, D), angle of failure (B, E) and mechanical stiffness (C, F) of contralateral non-fractured (A, B, C) and fractured (D, E, F) femora of WT controls (n = 13), Tac1 −/− (n = 10) and sympathectomized (6-OHDA application) mice (n = 12) 21 days after fracture setting. Comparison of stabilized fractured femora with contralateral, non-fractured femora of the same animal regarding resistance to torque (G), angle of failure (H) and stiffness (I) of wild type control (n = 13), Tac1 −/− (n = 10) and sympathectomized mice (n = 12) 21 days after fracture setting calculated in percent (values from non-fractured legs were set as 100%). Results are shown as mean ± SD; * $p < 0.05$; ** $p < 0.01$.

to WT (Fig. 4D). Fractured femora of Tac1 −/− mice have a significantly higher angle of failure than fractured femora of WT mice. There was no difference between fractured femora of sympathectomized to Tac1 −/− mice and WT (Fig. 4E). We found no significant differences in the mechanical stiffness of fractured femora between the three groups (Fig. 4F).

In addition, we related the mechanical properties of fractured femora to the respective contralateral non-fractured femora of the same animal calculated in percent of properties of non-fractured femora (set to 100%). When compared to contralateral non-fractured femora, the bone of fractured legs demonstrated similar torsional load, bending force and mechanical stiffness in WT control (Fig. 4G), Tac1 −/− (Fig. 4H) and sympathectomized mice (Fig. 4I).

2.8. μCT-analysis of bone architecture after fracture

μCT-analysis of the hard callus at day 21 past fracture only revealed alterations by trend in bone micro-architecture and structure between the groups (Supplementary Fig. 3A–E). Even though the fractured femora were stabilized intramedullary, callus size varied within the groups which resulted in high standard deviation obscuring potential statistical significant differences.

Besides the callus volume of interest (VOI) a proximal site to fracture callus was defined (Fig. 6F) and for this VOI the trabecular parameters were calculated, compared between groups, and compared between the fractured and non-fractured site.

In proximal sites of fractured legs, sympathectomized mice had a lower trabecular number compared to Tac1 −/− and WT (Fig. 5A), while trabecular separation is higher than in Tac1 −/− mice (Fig. 5C). Both trabecular parameters were altered by trend in Tac1 −/− mice. Trabecular thickness was not different between the three groups (Fig. 5B). Connectivity-density and bone mass was profoundly decreased in sympathectomized mice in comparison to Tac1 −/− and WT (Fig. 5D, E) whereas these parameters were increased in Tac1 −/− mice compared to WT (Fig. 5D) and to sympathectomized mice (Fig. 5E).

Notably, for the contralateral proximal femur, both the sympathectomized mice and Tac1-deficient mice had lower trabecular number and trabecular thickness compared to WT (Fig. 5F, G) whereas trabecular separation was profoundly higher (Fig. 5H). With respect to trabecular connectivity and bone mass parameters, sympathectomized mice and Tac1-deficient mice had a profound lower degree of trabecular connectivity and bone mass compared to WT (Fig. 5I, J).

We compared the structural parameters of VOIs proximal to fracture site with the corresponding proximal VOIs in contralateral, unfractured legs (100% line) within each mouse group (Fig. 6A–E). In the WT control mice, trabecular number (Fig. 6A), trabecular thickness (Fig. 6B), connectivity (Fig. 6D) and bone mass (Fig. 6E) were significantly reduced in VOIs proximal to fracture site compared to contralateral non-

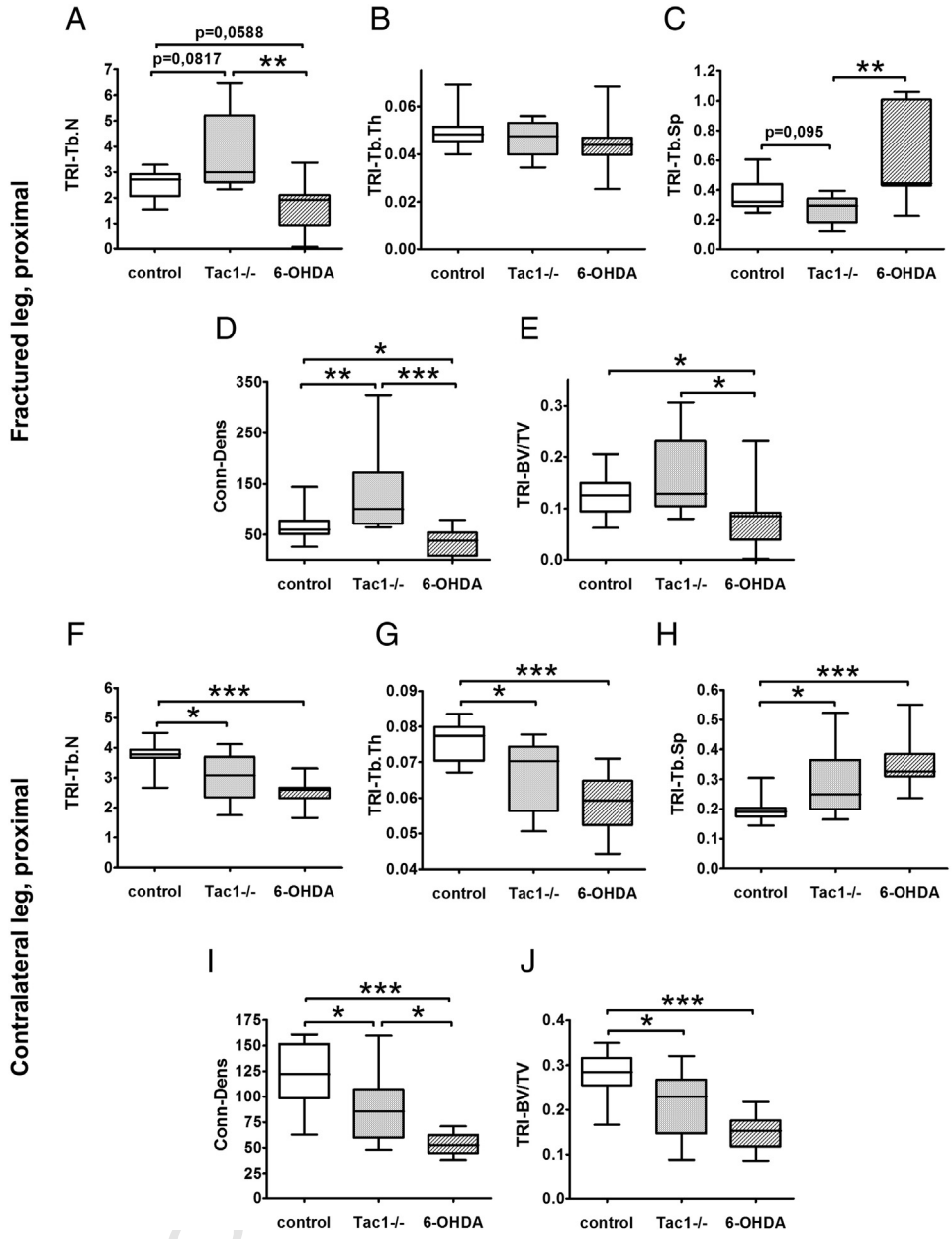

Fig. 5. µCT-analysis of trabecular bone proximal to the fracture site and of the contralateral, non-fractured leg. Comparison of trabecular number (Tb.N) (A, F), trabecular thickness (Tb.Th) (B, G), trabecular separation (Tb.Sp) (C, H), connectivity density (Conn.-Dens) (D, I) andbone mass (BV/TV) (E, J) of trabecular bone proximal to the fracture site of fractured femora (A–E) and proximal trabecular bone of non-fractured contralateral femora (F–J) of WT control (n = 12), Tac1 −/− (n = 9) and sympathectomized mice (6-OHDA application) (n = 8) 21 days after setting intramedullary stabilized fractures in left femora. Data are shown as mean ± SD; * $p < 0.05$; ** $p < 0.01$; *** $p < 0.001$.

fractured femur while trabecular separation (Fig. 6C) was increased. In the Tac1 −/− mice, only the trabecular thickness (Fig. 6B) was reduced in VOIs proximal to the fracture site compared to VOIs in contralateral legs. All other parameters were unaffected. In sympathectomized mice the structural bone parameters of VOIs proximal to fracture site did not differ to VOIs in contralateral legs.

2.9. Touch sensitivity in fractured and unfractured legs

We measured touch sensitivity of non-fractured right legs to investigate whether pain sensation was altered in Tac1 −/− and sympathectomized mice before fracturing. We were unable to detect significant differences of healthy right legs in control, Tac1 −/− and sympathectomized mice before (day 0) and on days 5 and 8 after fracturing (Fig. 7A).

At 5 days after fracture, Tac1 −/− mice had a higher pressure threshold in fractured legs compared to WT and sympathectomized mice. There was no difference regarding touch sensitivity in fractured legs between sympathectomized and WT animals at this time point. At 8 days after fracture, sympathectomized mice had a higher pressure threshold in fractured legs than WT and Tac1 −/− mice (Fig. 7B).

2.10. Analysis of locomotion

To exclude the possibility that modifications of the genetic background (Tac1 −/−) or 6-hydroxy dopamine (6-OHDA) application generally alters mouse locomotion, WT, Tac1 −/− and sympathectomized mice were tracked for 1 h separately in their home cages. Totally moved distance and the mean movement velocity were analyzed. No differences in total distance moved [cm] or mean velocity [cm/s] between the groups during the 1 h period could be observed (Fig. 7C and D) pointing to an equal mechanical load bearing behavior prior to fracture setting.

Please cite this article as: Niedermair, T., et al., Absence of substance P and the sympathetic nervous system impact on bone structure and chondrocyte differentiation in an adult mod..., Matrix Biol. (2014), http://dx.doi.org/10.1016/j.matbio.2014.06.007

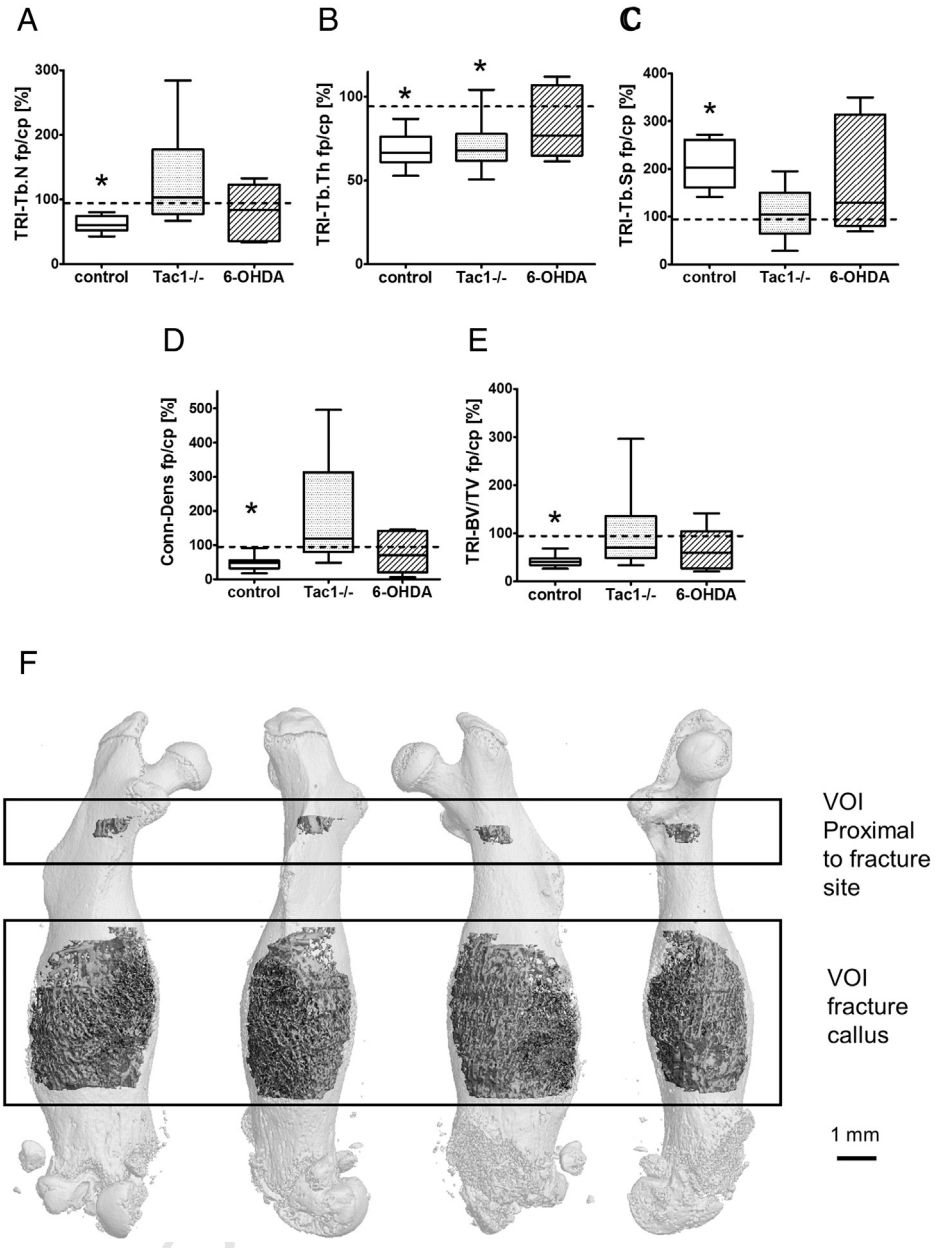

Fig. 6. Relation of structural bone parameters of fractured to non-fractured contralateral femora and μCt images of a fractured femora representing volumes of interests (VOIs). Tb.N. (A), Tb.Th (B), Tb.Sp (C), Conn.-Dens (D) and BV/TV (E) of trabecular bone proximal to the fracture site of fractured femora were related to corresponding trabecular bone of contralateral femora in control, Tac1 −/− and sympathectomized (6-OHDA application) (A–E) mice. Structural parameters of VOIs proximal to fracture site of fractured femora were normalized to VOIs of contralateral femora. Values obtained from non-fractured contralateral femora were set as 100%. Representative μCt images of the left femora of a Tac1 −/− mouse 21 days after setting intramedullary stabilized fractures (F). Analyzed volumes of interest (VOI) within the callus region after fracture repair, and the proximally/trochanteric placed trabecular placement for comparison purpose of side differences, in a transparently presented femur. From left to right: posterial, lateral, frontal and medial view. Dark gray labeled areas represent VOIs. Scale bar = 1 mm.

3. Discussion

In this study, we analyzed the impact of the absence of SP, a major sensory neurotransmitter, and the absence of the SNS on callus differentiation and bone remodeling as a model of endochondral differentiation during skeletal growth in adults. We detected SP-, NK1R- and TH-immunoreactive nerve fibers at the fracture site early after fracture setting. TH-positive nerve fibers remained present at the fracture site, however became displaced to the callus periphery not invading the cartilaginous callus but the periosteum which is in agreement with an earlier report (Li et al., 2001). SP-positive nerve fibers disappeared within the first days from the fracture site. Instead, we detected SP- and NK1R positive callus cells early after fracture with increasing numbers during formation of a cartilaginous callus. This is in analogy to an observation of Capellino et al., who described that in experimental arthritis catecholaminergic SNF disappeared from the synovium around the onset of the disease but were soon after replaced by TH-positive synovial cells. These cells were present only in inflamed synovial tissue which indicates that modulation of locally produced catecholamines has strong anti-inflammatory effects in vivo and in vitro (Capellino et al., 2010). We observed no TH-positive callus cells indicating that effects of catecholamines were transmitted by respective nerve fibers in neighboring tissues, i.e. periosteum. However, callus cells were immunoreactive for α1d- and α2b-adrenoceptors and thus perceptible for catecholaminergic neurotransmitters. We demonstrated previously that costal chondrocytes of neonatal mice are able to respond to neuronal mediators of the sensory and catecholaminergic sympathetic system as they express adequate receptors (Opolka et al., 2012).

Please cite this article as: Niedermair, T., et al., Absence of substance P and the sympathetic nervous system impact on bone structure and chondrocyte differentiation in an adult mod..., Matrix Biol. (2014), http://dx.doi.org/10.1016/j.matbio.2014.06.007

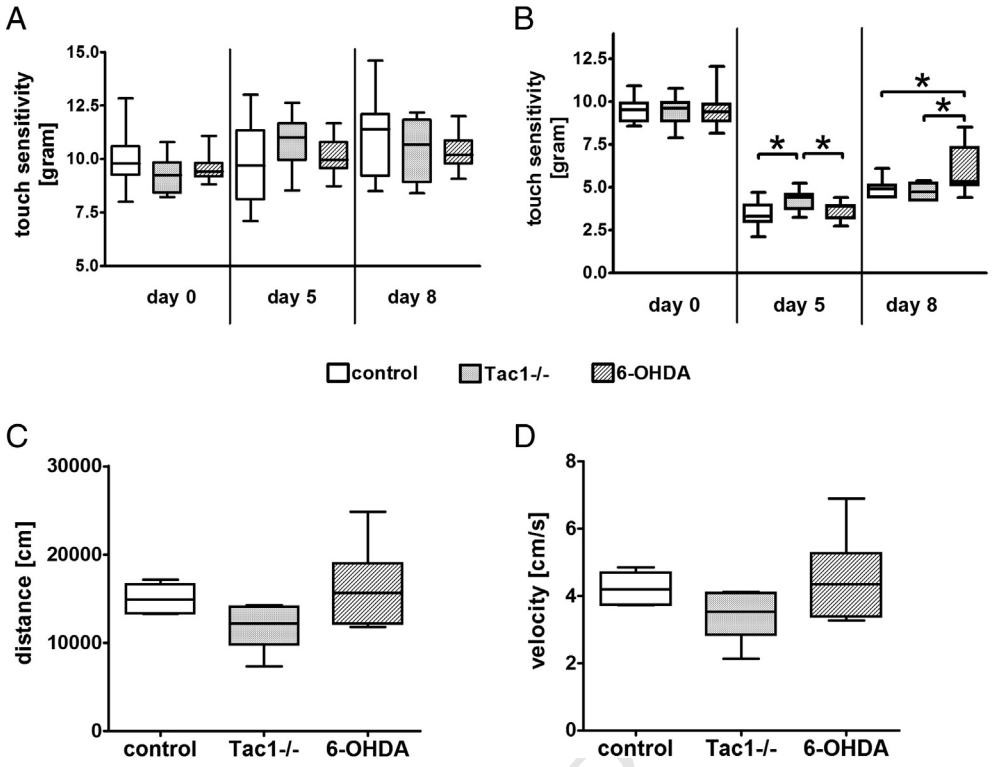

Fig. 7. Aesthesiometer test for touch sensitivity and behavioral test for locomotion. Touch sensitivity was measured in left and right hind legs before (day 0) and on days 5 and 8 after setting fractures in WT control (n = 10), Tac1 −/− (n = 15) and sympathectomized mice (6-OHDA application) (n = 12). (A) Touch sensitivity (in gram) in non-fractured contralateral right hind legs before setting fractures (day 0) and on day 5 and 8 after setting fractures. (B) Touch sensitivity (in gram) in fractured left hind legs directly before (d 0) and 5 and 8 days after fracture. Comparison of the total distance moved [cm] (C) and the mean velocity [cm/s] (D) of WT controls (n = 6), Tac1 −/− (n = 6) and sympathectomized mice (n = 6) during 1 h video tracking in separated home cages. Data are shown as mean ± SD; * $p < 0.05$.

Fracture callus of sympathectomized mice consists of a higher proportion of mesenchymal callus tissue and a lower proportion of cartilaginous callus tissue early after fracture suggesting that the absence of sympathetic neurotransmitters delays differentiation of mesenchymal callus tissue toward a cartilaginous matrix. This observation corresponds to in vitro data which demonstrate that norepinephrine (NE) stimulation of mesenchymal stem cells (MSC), kept in micromass pellets, dose-dependently inhibits chondrogenic differentiation via ß-adrenoceptors as chondrogenic MSC aggregates treated with NE or isoproterenol (ß-adrenoceceptor agonist) synthesized lower amounts of type II collagen and glycosaminoglycans (Jenei-Lanzl et al., 2014). Notably, the absence of both SP and the SNS reduce callus area positive for hypertrophic chondrocytes in the late phase of callus remodeling where matrix mineralization starts and the hard callus is formed. This effect is according to in vitro data which demonstrate that NE accelerates hypertrophic differentiation by inducing hypertrophic markers collagen X and MMP-13 in chondrogenically differentiated MSC (Jenei-Lanzl et al., 2014). We demonstrated previously, that stimulation of murine costal chondrocytes kept in micromass pellets with SP temporarily induces *mmp-13* gene expression whereas *col10a1* gene expression was unaffected (Opolka et al., 2012).

After abolishing sympathetic influence on bone metabolism one would expect a high bone mass phenotype (HBM) as seen in studies using β2-adrenergic receptor deficient or Leptin deficient mice (Takeda et al., 2002; Elefteriou et al., 2005). In contrast, we found that torsional failure load, bending force and stiffness were reduced in the absence of the SNS implying inferior bone quality compared to normal innervated bone. Results of μCt analyses corroborated the inferior mechanical bone quality as trabecular bone from sympathectomized mice had reduced numbers of trabecula compensated by an increase in trabecula separation. Also bone mass, density and trabecular connectivity were reduced. We found a similar but even more pronounced situation in the contralateral non-fractured leg where additional trabecula thickness was strongly reduced. A major reason for that observation appears to be an increase of bone resorption as we observed a higher number of TRAP-positive osteoclasts populating the fracture callus after sympathectomy but no change of osteoblast number. In comparison to WT we found that osteoclasts of sympathectomized mice differentiated in vitro from bone marrow derived macrophages (BMM) seem to be more active due to a lower apoptosis rate as cells isolated from Tac1 −/− mice. We detected a higher ALP activity in osteoblasts isolated from sympathectomized mice compared to osteoblasts isolated from Tac1 −/− mice which may in turn activate additional osteoclasts through increased expression of RANKL. We suggest the following mechanisms to contribute to this unexpected bone phenotype. Norepinehrine (NE) and epinephrine (E) content in sympathectomized animals is reduced by 80% leaving very low NE/E concentrations which then act primarily via α-adrenergic receptors as affinity of NE/E for α-adrenoceptors is profoundly higher than for ß-adrenoceptors (Harle et al., 2005; Straub et al., 2006). Expression of α-adrenergic receptors was demonstrated in osteoblasts and osteoclasts (Togari, 2002; Nishiura and Abe, 2007). Binding of NE/E to α_1-adrenergic receptors stimulates RANKL expression and release from osteoblasts which is a potent activator of osteoclastogenesis of progenitor cells (Nishiura et al., 2007). In this line, inactivation of α_{2A}- and α_{2C}-adrenoceptors increased bone formation and decreased bone resorption whereas stimulation with an α_2-adrenergic agonist increased osteoclast formation (Fonseca et al., 2011). Therefore, we propose that the remaining low concentrations of these catecholamines stimulate osteoclastogenesis by directly binding to osteoclast precursor cells and thus increasing osteoclast differentiation. In a second, indirect way, they may increase osteoclastogenesis by inducing RANKL expression and release in osteoblasts. Besides, Sherman and Chole proposed a mechanism where selective destruction of noradrenergic and dopaminergic SNF by applying the neurotoxic false neurotransmitter 6-hydroxydopamin (6-OHDA) increased sensory uptake of nerve growth factor (NGF) normally required

Please cite this article as: Niedermair, T., et al., Absence of substance P and the sympathetic nervous system impact on bone structure and chondrocyte differentiation in an adult mod..., Matrix Biol. (2014), http://dx.doi.org/10.1016/j.matbio.2014.06.007

by SNF for maintenance and survival followed by osteoclast induction. Capsaicin, a sensory specific neurolytic compound, eliminates this in vivo osteoclast-inductive effects of 6-OHDA when applied 12 h before treatment (Sherman and Chole, 1995). We propose that sensory NGF uptake might shift the balance to increased SP release by sensory neurons and thereby contributing to increased osteoclast numbers and activity. Importantly, bone resorption requires a profound shorter time span compared to bone formation, it takes at least 3 months to rebuild an area of bone resorbed by osteoclasts in 2–3 weeks (Harada and Rodan, 2003). Thus, increased bone resorption, even when accompanied by coupled increased bone formation, can cause bone loss owing to these kinetic differences. Therefore, we propose that the absence of SNS immediately induces bone resorption without significantly affecting bone formation during our experimental time line of 4 weeks culminating in netto bone degradation (Fig. 8, right panel).

Impaired mechanical bone properties were demonstrated when reduced levels of SP were detected at the fracture site after ovariectomy (Ding et al., 2010). This is in line with our data showing altered mechanical bone properties of Tac1 −/− mice as reduced resistance to torque and bone stiffness and increased angel of failure in addition to reduced bone structural parameters. By blocking the NK1R chemically for 2 weeks, Kingery and colleagues reported significant reduction in bone mineral density suggesting a role for SP in maintaining bone integrity and regulation of bone formation (Kingery et al., 2003). However, some studies reported controversial effects on bone formation for SP depending on its concentration. While SP concentration >10–8 M stimulates osteoblast differentiation and matrix mineralization (Goto et al., 2007; Wang et al., 2009), SP concentration <10–8 M blocks osteoblast differentiation (Adamus and Dabrowski, 2001). In addition, SP stimulates the proliferation of osteoblast precursor cells (Wang et al., 2009) and other cells, i.e. chondrocytes (Opolka et al., 2012) in a concentration dependent manner. We observed higher apoptosis rate in osteoblasts derived from BMM isolated from Tac1-deficient mice and in three out of four Tac1 −/− animal osteoblast numbers in fracture callus were reduced about 50%. These data indicate a positive effect of SP on bone formation if high concentrations of SP are available and a negative effect if SP concentration is low or if the neuropeptide is absent. However, we also observed a reduced number of osteoclasts at the fracture site in Tac1-deficient mice which maybe due to higher apoptosis rate as we measured a higher apoptosis rate in osteoclasts differentiated from BMM isolated from Tac1-deficient mice in vitro. This is in line with a study of Hill et al. who reported a decrease in osteoclast-occupied mandibular bone surface after neonatal capsaicin treatment (Hill et al., 1991). This strengthens the theory that SP can additionally act as a bone catabolic factor increasing bone resorption by inducing osteoclastogenesis (Wang et al., 2009) and resorptive activity of osteoclasts (Kojima et al., 2006). We suggest that the absence of SP signaling in Tac1-deficient mice leads to inferior bone parameters due to a priori

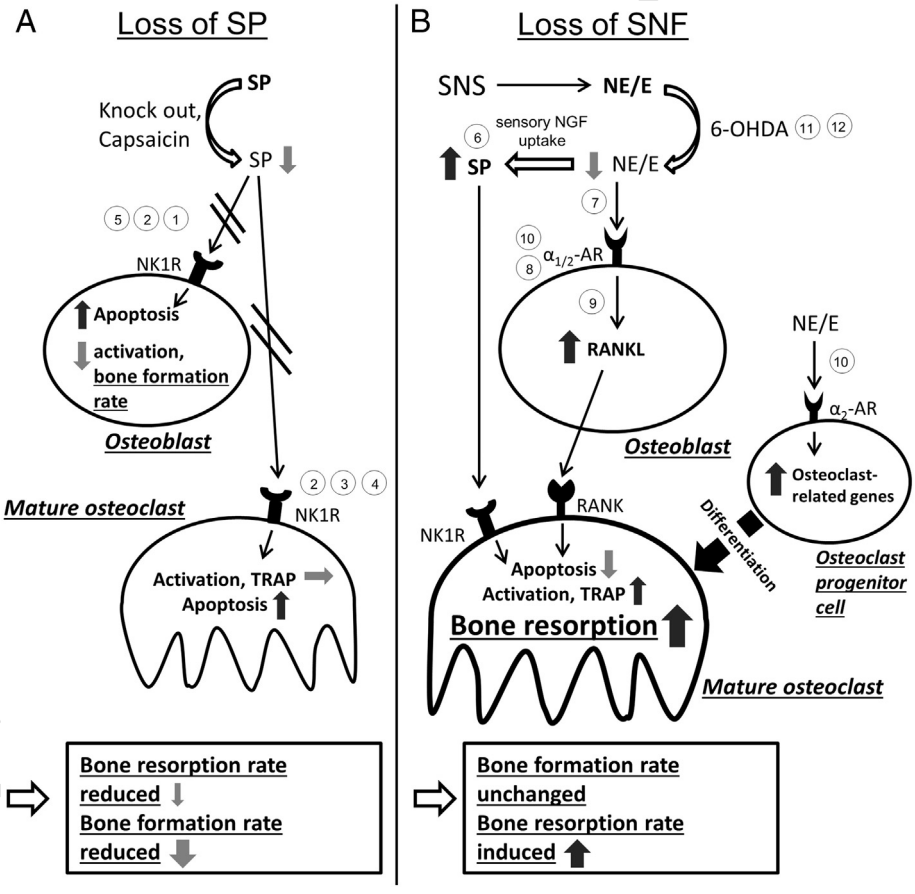

Fig. 8. Summary of proposed mechanisms responsible for altered structural bone parameter. (A) Absence of SP: Absence of SP signaling via NK1R induces apoptosis but has no influence on number and resorption activity of osteoclasts thereby leading to a reduced bone resorption rate. It also induces osteoblast apoptosis and reduces activity resulting in a net decrease in bone formation rate during skeletal growth when SP is absent (left panel). (B) Absence of sympathetic nerve fibers (SNF): 6-OHDA treatment selectively destroys catecholaminergic nerve fibers and strongly reduces catecholaminergic neurotransmitter concentrations. Low concentrations of catecholaminergic neurotransmitters norepinephrine/epinephrine (NE/E) act via α-adrenergic receptors on osteoblasts increasing RANKL expression and release, and on osteoclast progenitor cells inducing upregulation of osteoclastogenesis-related genes and subsequently increasing osteoclast differentiation rate. In addition, sensory NGF uptake might lead to increased SP release and concomitantly augments osteoclast activation via the NK1R. Together, these mechanisms lead to increased osteoclast differentiation and activation and a net increase in short time bone resorption while bone formation presumably remains unchanged (right panel). 1) Adamus et al., J Cell Biochem 2001; 2) Wang et al., BONE 2009; 3) Hill et al., Neuroscience 1991; 4) Kojimata et al., Inflamm Res 2006; 5) Goto et al., Neuropeptides 2007; 6) Sherman and Chole, Otolaryngol Head Neck Surg 1995; 7) Härle et al., Arthritis & Rheumatism 2005; 8) Togari et al., Microsc Res Tech 2002; 9) Nishiura and Abe, Arch Oral Bio, 2007; 10) Fonseca et al., JBMR 2011; 11) Sachs and Jonsson, Biochemical Pharmacology 1975; 12) Rodriguez-Pallares et al., JNC 2007.

Please cite this article as: Niedermair, T., et al., Absence of substance P and the sympathetic nervous system impact on bone structure and chondrocyte differentiation in an adult mod..., Matrix Biol. (2014), http://dx.doi.org/10.1016/j.matbio.2014.06.007

reduced netto bone formation rate which is not balanced by in parallel reduced osteoclastogenesis and thus reduced bone resorption (Fig. 8, left panel).

We observed an increased touch sensitivity of Tac1-deficient and sympathectomized mice. SP, a critical nociceptive neurotransmitter mediates pain behavior after fracture (Li et al., 2012). It was demonstrated that fracturing increased SP gene expression in the ipsilateral dorsal root ganglion and neuropeptide protein levels in the sciatic nerve (Wei et al., 2009). Thus it can be expected that lack of substance P will have an effect on pain transmission. In addition, sympathectomy leads to an increased touch sensitivity which might be due to involvement of the SNS in pain transmission and behavior (Straub, 2011). When relating structural bone parameters of fractured femora to contralateral, unfractured femora, we observed altered structural parameters in fractured legs of WT animals as reduced bone mass and trabecula numbers and thickness. When related to non-fractured legs, these structural parameters were not altered in Tac1-deficient mice and mice without SNS. We demonstrated that unchallenged Tac1 −/− mice and mice without SNF displayed no change in locomotion and mobility. So we suggest that due to a reduced touch sensitivity, mice experience less pain at the fracture site and thus they do not hesitate to put equal load on both legs already early after fracture whereas WT mice spare their fractured legs. Prolonged reduced load supposedly quickly alters bone turnover and remodeling during the healing process not only directly at the fracture site but also in regions proximal to the callus. To our surprise, bone micro-architecture was more impaired proximal to the fracture site in fractured legs of WT and sympathectomized mice compared to Tac1-deficient mice. This might be explained by the reduced pain sensitivity in Tac1-deficient mice early after fracture presumably resulting in equal load bearing of both legs already in the inflammatory phase of fracture healing. We assume that WT and sympathectomized mice spare fractured legs for a longer time compared to Tac1 −/− mice thus bone turnover and remodeling are more intensely altered in their fractured legs.

As all in all structural bone parameters of fractured femora after sympathectomy were not only altered compared to WT but also to Tac1-deficient mice, we suggest a more pronounced influence of the whole SNS on bone remodeling as SP alone. For contralateral femora of Tac1-deficient mice, structural parameters were similarly altered as for sympathectomized mice, however less pronounced, indicating partly similar effects (but milder for SP) of both nervous systems on bone architecture.

4. Conclusion

SP and the SNS are important neuronal effectors regulating bone formation and resorption after trauma and during skeletal growth. Structural bone properties are impaired in fractured and non-fractured legs of Tac1-deficient and sympathectomized mice which is more pronounced in non-fractured legs in the absence of SP and even more so when sympathetic nervous stimuli are missing. We suggest that the absence of SNS impacts a priori on bone structural parameters by increasing immediately bone resorption and that appropriate sensory neurotransmitter supply is mainly needed for proper bone formation during skeletal growth. Of note, both neuronal systems reduce pain sensation after fracture trauma.

In addition, to affect bone remodeling, the absence of SNS delays callus maturation at an early time point after fracture whereas lack of SP does not. However, the absence of SP and SNS modulates callus differentiation by delaying hypertrophic differentiation of chondrocytes suggesting a pro-differentiation effect in the late phase of callus remodeling representative for endochondral ossification during skeletal growth.

We suggest that initial SP release by nerve fibers at the fracture site might later be replaced by endogenously produced SP from resident callus chondrocytes.

All in all, we propose that sensory and sympathetic neurotransmitters have crucial trophic effects which are essential for proper bone formation and remodeling in addition to their classical neurological actions.

5. Methods

5.1. Animal models

A tachykinin 1(Tac1)-deficient mouse strain was used in order to better characterize the effects of SP loss on bone regeneration and properties of newly formed bone. The Tac1 knockout mouse strain harboring a targeted mutation in the *Tac1* gene on a C57Bl6 background was described previously (Zimmer et al., 1998; Guo et al., 2012). In addition, the SNS was destroyed by chemical sympathectomy in order to characterize effects of sympathetic neurotransmitters on bone regeneration. C57Bl6/J mice (Charles River, Sulzfeld, Germany) were randomly divided into a control group and a sympathectomized group. For sympathectomy, 6-hydroxydopamine (6-OHDA, Sigma, Steinheim, Germany, 80 μg/g bodyweight) was injected i.p. on days 8, 7 and 6 prior to fracture setting reducing the production of adrenergic neurotransmitters about 80% (Sachs and Jonsson, 1975; Harle et al., 2005). Animals were kept under standardized conditions with free access to food and water.

5.2. Fracture models

Fractures were set in 8–10 weeks old male mice which was in agreement with the local veterinary administration and in accordance to the ethical committee and local authorities controlling animal experimental usage (Az: 0.54-2532.1-26/10).

Mice were anesthetized by intraperitoneal (ip) injections of 90–120 mg ketamine (Ketamine 10%, Garbsen, Germany) and 6–8 mg xylazine (Xylazine 2% Bernburg, Bernburg, Germany) per kg bodyweight.

For mechanical testing and μCT-analysis, the left femora were subjected to closed standardized mid-diaphyseal fractures as previously described (Holstein et al., 2007). The left femora were fractured with a fracture machine by three-point bending (modified from protocol described by Bertrand et al. (Bertrand et al., 2013)) and flexible stabilized with an intramedullar nail. Buprenorphinhydrochloride (Temgesic, Essex Pharma GmbH, München, Germany, 0.1 μg/g bodyweight) was given s.c. immediately after surgery and the following 2 days. After 21 days mice were euthanized and fractured and contralateral legs were immediately frozen at −20 °C.

Non-stabilized tibia fractures were used for all other experiments. A closed transverse fracture was created in the distal part of the diaphysis of the left tibia by manual three-point bending without further stabilization. Mice were euthanized at different time points as indicated.

5.3. Behavioral test for locomotion

To test for differences in locomotion, WT, Tac1 −/− and sympathectomized mice (prior to fracture setting) were set separately in new home cages and monitored for 1 h with a video camera (Sony DCR-HC90E; The Heights, Brooklands, UK). The video tracking software EthoVision XT 7 (Noldus Information Technology, Wageningen, Netherlands) was used to analyze the total distance moved [cm] and mean velocity [cm/s] during the 1 h tracking period. Sympathectomy with 6-OHDA (80 mg/kg KG) was performed on day -8, -7 and -6 prior to video tracking.

5.4. Dynamic Plantar Aesthesiometer test for touch sensitivity

Touch sensitivity was measured in both hind paws before and after setting tibia fractures (Dynamic Plantar Aesthesiometer, Ugo Basile, Comerio, Italy). Each mouse was placed on a mesh in a separated

Please cite this article as: Niedermair, T., et al., Absence of substance P and the sympathetic nervous system impact on bone structure and chondrocyte differentiation in an adult mod..., Matrix Biol. (2014), http://dx.doi.org/10.1016/j.matbio.2014.06.007

compartment. A von Frey filament was placed under the center of one of the hind paws. The electric actuator was started to lift up the filament with increasing force (gram) until the mouse withdraws the paw. Tests were carried out on days 5, 3 before and at the day of fracturing and on days 5 and 8 after fracture. In each test, three values were recorded for each paw and averaged. Values measured 5 and 8 days after fracture were related to values before fracturing.

5.5. Sample preparation for histology and immunohistology

Fractured tibiae were dissected on days 5, 9 and 13 after fracture and fixed in freshly prepared paraformaldehyde in PBS at 4 °C for 24 h. Bones were decalcified in 20% ethylene diaminetetraacetic acid (EDTA; Roth, Karlsruhe, Germany), pH 7.3, for 4 weeks. After dehydration through a graded series of ethanol solutions, fractured tibiae were embedded in paraffin. 5 μm sections were cut through the long axis of embedded tibiae.

5.6. Immunofluorescence staining

Deparaffinized and rehydrated sections were incubated in 3% hydrogen peroxide (Roth). Sections, stained for SP, NK1R and TH were blocked in 5% bovine serum albumin (Roth) in PBS for 1 h at room temperature (RT). For adrenergic receptor staining, sections were pre-incubated in 0.05% protease XXIV and 0.1% hyaluronidase(both Sigma-Aldrich, Taufkirchen, Germany) at 37 °C. Blocking was performed in 10% normal goat serum (NGS) in PBS for 20 min at RT. Immunofluorescence was performed with primary antibodies against SP (Santa Cruz, Heidelberg, Germany, sc-21715, dilution 1:100), NK1R (Chemicon, Schwalbach, Germany, AB5060, dilution 1:250) and TH (Chemicon, AB152, dilution 1:100), incubated over night in blocking solution at 4 °C. Primary antibodies for α1d (Alamone Labs, Jerusalem, Israel, AAR-019, dilution 1:100), α2b (Alamone Labs, AAR-021, dilution 1:100) and β2 (abcam, Cambridge, UK, ab36956, dilution 5 μg/ml) were incubated in 1% NGS over night at 4 °C. Secondary antibodies (Invitrogen, Karlsruhe, Germany), conjugated to Alexa Fluor 488 (SP, TH, adrenergic receptors) and Alexa 568 (NK1R), were used for detection. Nuclei were stained with DAPI (Invitrogen) and slides were finally embedded in Fluorescent Mounting Media (Dako North America, Inc., Carpinteria, CA). SP, NK1R, TH and adrenergic receptor stainings were photographed using an Olympus BX61microscope (Olympus Deutschland GmbH, Hamburg, Germany) with a 40-fold magnification. Staining specificity was controlled by incubating sections without the first antibodies (negative controls).

5.7. Immunohistochemistry

Mouse anti-collagen X (diluted 1:25; Quartett, Berlin, Germany) and mouse anti-RUNX2 (diluted 1:50; ab76956, Abcam, Cambridge, UK) were used together with the DAKO® Animal Research Kit (Dako North America, Inc., Carpinteria, CA, USA). Deparaffinized, rehydrated sections were incubated in 3% hydrogen peroxide and prior to antibody staining sections were treated with 0.05% protease XXIV(Sigma-Aldrich) and 0.1% hyaluronidase(Sigma-Aldrich) at 37 °C. Primary antibodies were incubated for 15 min at RT according to the protocol of DAKO® Animal Research Kit followed by incubation with Streptavidin-HRP. Finally sections were incubated with DAKO® Liquid Substrate System. Nuclei were stained with Weigert's hematoxylin, and slides were embedded with Depex®. Sections of growth plate served as positive controls. Staining specificity was controlled by incubating sections without the first antibodies (negative controls).

5.8. Osteoclast staining

The Acid Phosphatase, Leukocyte Kit (Sigma-Aldrich, Taufkrichen, Germany, 387A-1KT) was used to stain tartrate resistant acid phosphatase (TRAP) characteristic for osteoclasts. Staining procedure was conducted with deparaffinized and rehydrated sections. Overview images were scanned with the TissueFAXSi plus system (TissueGnostics, Vienna, Austria).

5.9. Morphometrical analysis

From every fractured tibia three sagittal paraffin sections with an intersection distance of 150 μm were stained with Weigert's hematoxylin (Merck, Darmstadt, Germany), Alcian blue (Serva, Heidelberg, Germany) and Sirius red (Sigma-Aldrich, Taufkirchen, Germany). Overview images were photographed (Olympus BX61; 20× magnification) and analyzed using Adobe Photoshop CS4. Total callus area, cartilaginous and calcified areas as well as non-stained areas within sections (loss of tissue due to staining procedure) were determined as regions of interests. Number of pixel was quantified to calculate proportion of cartilaginous, calcified and non-stained areas in relation to total callus area. The remaining tissue was regarded as mesenchymal callus tissue and calculated by subtracting pixel number of cartilaginous callus area, calcified callus area and non-stained areas from total callus area.

From day 13, consecutive sections were stained with mouse anti-collagen X. Pixel number of collagen X stained area was determined and pixel number of cartilaginous callus (determined in Alcian blue/Sirius red stained sections) was used to calculate the proportion of the area of hypertrophic chondrocytes in the cartilaginous callus. Results of WT mice were set as 100% and data from sympathectomized and Tac1 −/− mice were related to controls.

To determine the number of osteoclasts per mm^2 in calcified callus tissue at day 13 after fracture, the area of calcified callus (mm^2) was determined as region of interest (HistoQuest software, TissueGnostics). The total number of osteoclasts in regions of interests was counted and number of osteoclasts/mm^2 was calculated.

Osteoblast numbers were determined at day 13 after fracture by counting RUNX2 positive stained nuclei. Osteoblast number was determined by taking 10 pictures of different callus areas (mesenchymal, soft and hard callus tissue) with the Nikon C1 confocal microscope (60× magnification with oil; Nikon, Düsseldorf, Germany). RUNX2-positive stained cells were counted, values of control mice were set as 100%.

5.10. Primary bone marrow macrophage and osteoblast isolation

BMM and osteoblasts were isolated according to standard protocols with minor modifications (Dillon et al., 2012). Briefly, long bones were removed, cleaned and washed in PBS. Epiphyses were cut off, bone marrow was flushed out with medium (αMEM, #M4526, Sigma-Aldrich, Taufkirchen, Germany) using a 27-gauge needle and BMM were pelleted by centrifugation. Erythrocytes were lysed by hypotonic shock. Cells were resuspended in medium supplemented with 10% FCS, 1% Pen/Strep, 2% GlutaMAX™-I (100×, #35050-38, Gibco Life Technologies, Darmstadt, Germany), 20 ng/ml M-CSF (#315-02, Peprotech, Hamburg, Germany) and cultured in petri dishes for 3 days. Long bones were cut into 2 × 2 mm pieces and washed with 2 mg/ml collagenase type II (Collagenase Type II, Worthington Biochemical Corp., Lakewood, USA) in medium (DMEM low glucose, #31885-023, Gibco Life Technologies, Darmstadt, Germany) at 37 °C two times for 20 min. Bone pieces were washed and cultured in petri dishes in medium supplemented with 10% FCS, 1% Pen/Strep and 100 μM ascorbic acid 2-phosphate (Sigma, Saint Louis, USA). Bone cells started to migrate out from bone chips and were then cultured until reaching confluency (15 ± 2 days).

5.11. Osteoclast differentiation, activity and apoptosis

For osteoclast differentiation BMM were detached (0.02% EDTA in PBS, 4 °C) after 3 days and seeded for 5 days in 96 well plates (5000 cells/well, triplicates) in α-MEM medium supplemented with 10% FCS,

Please cite this article as: Niedermair, T., et al., Absence of substance P and the sympathetic nervous system impact on bone structure and chondrocyte differentiation in an adult mod..., Matrix Biol. (2014), http://dx.doi.org/10.1016/j.matbio.2014.06.007

1% Pen/Strep, 2% GlutaMAX, 20 ng/ml M-CSF, 50 ng/ml RANKL (#315-11, Peprotech, Hamburg, Germany). Differentiation capacity was tested after 5 days by staining for TRAP as described before. Overview images were photographed using the TissueFaxSi plus system and number of osteoclasts (cells containing ≥3 nuclei) was counted. Apoptosis rate was determined after 5 days measuring Caspase-3/7 activity (Apo-ONE® Homogeneous Caspase-3/7 Assay, #G7791, Promega, Madison, USA). For analyzing osteoclast activity, cathepsin K enzyme activity was measured. After 5 days osteoclasts were cultured for 24 h under serum free conditions. Protein concentration of the supernatant was determined (Pierce™ BCA Protein Assay Kit, Thermo Scientific, Rockford, USA). Cathepsin K enzyme activity in the supernatant was determined using a protocol from (Wittrant et al., 2003). For all assays, values of control mice were set as 100%, results of Tac1 −/− and sympathectomized mice were calibrated to the WT controls.

5.12. Osteoblast proliferation, activity and apoptosis

Cells migrated out from bone chips were trypsinized and seeded in 96 well plates (5000 cells/well, triplicates) in osteogenic culture medium (αMEM, #22571-020, Gibco Life Technologies, Darmstadt, Germany) supplemented with 10% FCS, 1% Pen/Strep, 4 mM GlutaMax, 100 μM ascorbic acid2-phosphate, 10 mM β-glycerophosphate (#G9422, Sigma-Aldrich, Steinheim, Germany), 100 nM dexamethasone (#D2915, Sigma-Aldrich, Steinheim, Germany) for 7 days. Proliferation was analyzed using Cell Proliferation ELISA (BrdU, colorimetric, Roche Diagnostics GmbH, Mannheim, Germany). QuantiChrom™ Alkaline Phosphatase Assay Kit (DALP-250, BioAssay Systems, Hayward, USA) was used to measure ALP enzyme activity. Apoptosis rate was determined as described before measuring caspase-3/7 activity. Results of Tac1 −/− and sympathectomized mice were calibrated to controls (100%).

5.13. Biomechanical analysis

Non-fractured right femora and stabilized fractured left femora were used for biomechanical tests 21 days after setting fractures. Prior to biomechanical testing, frozen legs were thawed overnight at 4 °C. Metal pins were removed from the fractured femora. Non-fractured and fractured femora were placed into a vertical position in a clamping slide, cartilage covered surface of condyles were placed as anterior. The distal and proximal ends were cast into bone cement. The positioned femora were then placed into a torsion test machine (Fine- and electromechanical research workshop, University Hospital, Münster) with axial preload of 0.4 N. A constant force of 2 mm/min provided by a spindle driven material testing machine (Lloyd LR5K Plus,Lloyd Instruments, West Sussex, UK) was transformed into rotational movement by the torsion test machine and transmitted to the bones. The final point was complete loss of load-carrying ability. A computerized data-acquisition system (Spider 8/Catman®4.5, HBM, Darmstadt) collected the data. Torque, determined as Nmm, and torsion angle (angle of failure), determined as radian (rad; calculated to °; formula: x rad*(360°/2 × pi)), were registered as a function of time and torsional stiffness was calculated with a special Excel matrix as a quotient of torsion and maximal angle of failure. To compare the biomechanical quality of newly formed bone with the existing bone, the results of fractured femora for each animal were normalized to the results of contralateral non-fractured femora and shown as percentage [contralateral non-fractured = 100%].

5.14. μCt-analysis

Prior to scanning metal pins used for stabilization of fractures were removed to avoid image artifacts. The complete bone specimen were scanned frozen in a micro-computed tomography system (vivaCT40, Scanco Medical AG, Brüttisellen, Switzerland) using an isotropic nominal resolution of 12.5 μm. The x-ray tube was operated at 70 kVp and 114 μA with an integration time of 380 ms and 1000 projections. Three-dimensional μCT data were reconstructed as recommended by the manufacturer using a standard convolution back-scatter projection procedure. Images were filtered using a Gauss filter (sigma = 1.2, support = 1 voxel) and segmented using a global threshold of 22.4% of the maximum gray-value (Müller and Rüegsegger, 1997). These segmentation steps were applied to all analyzed VOIs. The VOIs were selected, firstly from the newly formed callus region, excluding the newly formed thin cortical shell and the femoral midshaft bone, and secondly, a trabecular volume within the trochanteric region (Fig. 6F).

Usually, the distal femur condyles are selected for trabecular structure analyses. Due to the fact, that this region was affected and destroyed by pinning in the fractured femur, the proximal trabecular region was selected for 3D structure analysis. For side difference analysis we compared the structural bone parameters within the determined VOIs proximal to fracture site compared to corresponding VOIs in contralateral non-fractured legs. Results of each fractured leg (proximal to fracture site) were normalized to the corresponding contralateral leg (proximal) within each group and calculated as percentage [contralateral proximal = 100%].

The following three-dimensional structural parameters were determined using a direct 3-D approach (Hildebrand et al., 1999) without any model assumptions required for 2D analysis, using software provided by the manufacturer: bone volume fraction (Tb.BV), bone volume density (BV/TV), trabecular number (Tb.N, 1/cm), trabecular thickness (Tb.Th, mm), trabecular separation (Tb.Sp, mm), connectivity density (Conn.D, $1/mm^3$), structure model index (SMI) (Hildebrand and Rüegsegger, 1997), degree of anisotropy (DA), and material density (mg HA/cm^3).

5.15. Statistical analysis

All data are represented as mean ± SD. Graph Pad Prism 5.0 software was used for statistical analysis. Although there are some multiple comparisons (number max. 2), Bonferroni adjustment was not applied due to the explorative nature of the study. Difference in medians was tested by two-tailed Mann–Whitney *U*-test and one-way ANOVA. Wilcoxon signed-rank test was used where WT was set to 100%. P values less than 0.05 were considered as significant.

Supplementary data to this article can be found online at http://dx.doi.org/10.1016/j.matbio.2014.06.007.

Acknowledgments

We thank Anja Pasoldt for her superior technical assistance. This work was supported by a BMBF grant assigned to SG and RHS (01EC1004D) as sub-project of the consortium “ImmunoPain”.

References

Adamus, M.A., Dabrowski, Z.J., 2001. Effect of the neuropeptide substance P on the rat bone marrow-derived osteogenic cells in vitro. J. Cell. Biochem. 81, 499–506.
Aitken, S.J., Landao-Bassonga, E., Ralston, S.H., Idris, A.I., 2009. Beta2-adrenoreceptor ligands regulate osteoclast differentiation in vitro by direct and indirect mechanisms. Arch. Biochem. Biophys. 482, 96–103.
Amling, M., Takeda, S., Karsenty, G., 2000. A neuro (endo)crine regulation of bone remodeling. Bioessays 22, 970–975.
Aro, H., 1985. Effect of nerve injury on fracture healing. Callus formation studied in the rat. Acta Orthop. Scand. 56, 233–237.
Bertrand, J., Stange, R., Hidding, H., Echtermeyer, F., Nalesso, G., Godmann, L., Timmen, M., Bruckner, P., Dell'Accio, F., Raschke, M.J., Pap, T., Dreier, R., 2013. Syndecan 4 supports bone fracture repair, but not fetal skeletal development, in mice. Arthritis Rheum. 65, 743–752.
Bjurholm, A., Kreicbergs, A., Brodin, E., Schultzberg, M., 1988a. Substance P- and CGRP-immunoreactive nerves in bone. Peptides 9, 165–171.
Bjurholm, A., Kreicbergs, A., Terenius, L., Goldstein, M., Schultzberg, M., 1988b. Neuropeptide Y-, tyrosine hydroxylase- and vasoactive intestinal polypeptide-immunoreactive nerves in bone and surrounding tissues. J. Auton. Nerv. Syst. 25, 119–125.
Bjurholm, A., Kreicbergs, A., Ahmed, M., Schultzberg, M., 1990. Noradrenergic and peptidergic nerves in the synovial membrane of the Sprague-Dawley rat. Arthritis Rheum. 33, 859–865.

Please cite this article as: Niedermair, T., et al., Absence of substance P and the sympathetic nervous system impact on bone structure and chondrocyte differentiation in an adult mod..., Matrix Biol. (2014), http://dx.doi.org/10.1016/j.matbio.2014.06.007

Capellino, S., Cosentino, M., Wolff, C., Schmidt, M., Grifka, J., Straub, R.H., 2010. Catecholamine-producing cells in the synovial tissue during arthritis: modulation of sympathetic neurotransmitters as new therapeutic target. Ann. Rheum. Dis. 69, 1853–1860.

Claes, L.E., Heigele, C.A., 1999. Magnitudes of local stress and strain along bony surfaces predict the course and type of fracture healing. J. Biomech. 32, 255–266.

Claes, L.E., Wilke, H.J., Augat, P., Rubenacker, S., Margevicius, K.J., 1995. Effect of dynamization on gap healing of diaphyseal fractures under external fixation. Clin. Biomech. (Bristol., Avon.) 10, 227–234.

Dillon, J.P., Waring-Green, V.J., Taylor, A.M., Wilson, P.J., Birch, M., Gartland, A., Gallagher, J.A. , 2012. Primary human osteoblast cultures. Methods Mol. Biol. 816, 3–18.

Ding, W.G., Zhang, Z.M., Zhang, Y.H., Jiang, S.D., Jiang, L.S., Dai, L.Y., 2010. Changes of substance P during fracture healing in ovariectomized mice. Regul. Pept. 159, 28–34.

Ducy, P., Amling, M., Takeda, S., Priemel, M., Schilling, A.F., Beil, F.T., Shen, J., Vinson, C., Rueger, J.M., Karsenty, G., 2000. Leptin inhibits bone formation through a hypothalamic relay: a central control of bone mass. Cell 100, 197–207.

Einhorn, T.A., 1998. The cell and molecular biology of fracture healing. Clin. Orthop. Relat. Res. S7–S21.

Elefteriou, F., Ahn, J.D., Takeda, S., Starbuck, M., Yang, X., Liu, X., Kondo, H., Richards, W.G., Bannon, T.W., Noda, M., Clement, K., Vaisse, C., Karsenty, G., 2005. Leptin regulation of bone resorption by the sympathetic nervous system and CART. Nature 434, 514–520.

Fonseca, T.L., Jorgetti, V., Costa, C.C., Capelo, L.P., Covarrubias, A.E., Moulatlet, A.C., Teixeira, M.B., Hesse, E., Morethson, P., Beber, E.H., Freitas, F.R., Wang, C.C., Nonaka, K.O., Oliveira, R., Casarini, D.E., Zorn, T.M., Brum, P.C., Gouveia, C.H., 2011. Double disruption of alpha2A- and alpha2C-adrenoceptors results in sympathetic hyperactivity and high-bone-mass phenotype. J. Bone Miner. Res. 26, 591–603.

Garcia-Castellano, J.M., Diaz-Herrera, P., Morcuende, J.A., 2000. Is bone a target-tissue for the nervous system? New advances on the understanding of their interactions. Iowa Orthop. J. 20, 49–58.

Goto, T., Yamaza, T., Kido, M.A., Tanaka, T., 1998. Light- and electron-microscopic study of the distribution of axons containing substance P and the localization of neurokinin-1 receptor in bone. Cell Tissue Res. 293, 87–93.

Goto, T., Nakao, K., Gunjigake, K.K., Kido, M.A., Kobayashi, S., Tanaka, T., 2007. Substance P stimulates late-stage rat osteoblastic bone formation through neurokinin-1 receptors. Neuropeptides 41, 25–31.

Guo, T.Z., Wei, T., Shi, X., Li, W.W., Hou, S., Wang, L., Tsujikawa, K., Rice, K.C., Cheng, K., Clark, D.J., Kingery, W.S., 2012. Neuropeptide deficient mice have attenuated nociceptive, vascular, and inflammatory changes in a tibia fracture model of complex regional pain syndrome. Mol. Pain 8, 85.

Harada, S., Rodan, G.A., 2003. Control of osteoblast function and regulation of bone mass. Nature 423, 349–355.

Harle, P., Mobius, D., Carr, D.J., Scholmerich, J., Straub, R.H., 2005. An opposing time-dependent immune-modulating effect of the sympathetic nervous system conferred by altering the cytokine profile in the local lymph nodes and spleen of mice with type II collagen-induced arthritis. Arthritis Rheum. 52, 1305–1313.

Harrison, S., Geppetti, P., 2001. Substance P. Int. J. Biochem. Cell Biol. 33, 555–576.

Hildebrand, T., Rüegsegger, P., 1997. Quantification of bone microarchitecture with the structure model index. Comput. Methods Biomech. Biomed. Eng. 1, 15–23.

Hildebrand, T., Laib, A., Müller, R., Dequeker, J., Rüegsegger, P., 1999. Direct three-dimensional morphometric analysis of human cancellous bone: microstructural data from spine, femur, iliac crest, and calcaneus. J. Bone Miner. Res. 14, 1167–1174.

Hill, E.L., Turner, R., Elde, R., 1991. Effects of neonatal sympathectomy and capsaicin treatment on bone remodeling in rats. Neuroscience 44, 747–755.

Holstein, J.H., Menger, M.D., Culemann, U., Meier, C., Pohlemann, T., 2007. Development of a locking femur nail for mice. J. Biomech. 40, 215–219.

Huang, H.H., Brennan, T.C., Muir, M.M., Mason, R.S., 2009. Functional alpha1- and beta2-adrenergic receptors in human osteoblasts. J. Cell. Physiol. 220, 267–275.

Hukkanen, M., Konttinen, Y.T., Santavirta, S., Paavolainen, P., Gu, X.H., Terenghi, G., Polak, J. M., 1993. Rapid proliferation of calcitonin gene-related peptide-immunoreactive nerves during healing of rat tibial fracture suggests neural involvement in bone growth and remodelling. Neuroscience 54, 969–979.

Hukkanen, M., Konttinen, Y.T., Santavirta, S., Nordsletten, L., Madsen, J.E., Almaas, R., Oestreicher, A.B., Rootwelt, T., Polak, J.M., 1995. Effect of sciatic nerve section on neural ingrowth into the rat tibial fracture callus. Clin. Orthop. Relat. Res. 247–257.

Imai, S., Matsusue, Y., 2002. Neuronal regulation of bone metabolism and anabolism: calcitonin gene-related peptide-, substance P-, and tyrosine hydroxylase-containing nerves and the bone. Microsc. Res. Tech. 58, 61–69.

Jenei-Lanzl, Z., Grässel, S., Pongratz, G., Kees, F., Miosge, N., Angele, P., Straub, R.H., 2014. Norepinephrine inhibits mesenchymal stem cell and chondrogenic progenitor cell chondrogenesis and accelerates chondrogenic hypertrophy. Arthritis Rheumatol.

Jones, K.B., Mollano, A.V., Morcuende, J.A., Cooper, R.R., Saltzman, C.L., 2004. Bone and brain: a review of neural, hormonal, and musculoskeletal connections. Iowa Orthop. J. 24, 123–132.

Kingery, W.S., Offley, S.C., Guo, T.Z., Davies, M.F., Clark, J.D., Jacobs, C.R., 2003. A substance P receptor (NK1) antagonist enhances the widespread osteoporotic effects of sciatic nerve section. Bone 33, 927–936.

Kojima, T., Yamaguchi, M., Kasai, K., 2006. Substance P stimulates release of RANKL via COX-2 expression in human dental pulp cells. Inflamm. Res. 55, 78–84.

Kondo, H., Takeuchi, S., Togari, A., 2013. beta-Adrenergic signaling stimulates osteoclastogenesis via reactive oxygen species. Am. J. Physiol. Endocrinol. Metab. 304, E507–E515.

Lerner, U.H., 2002. Neuropeptidergic regulation of bone resorption and bone formation. J. Musculoskelet. Nueronal Interact. 2, 440–447.

Li, J., Ahmad, T., Spetea, M., Ahmed, M., Kreicbergs, A., 2001. Bone reinnervation after fracture: a study in the rat. J. Bone Miner. Res. 16, 1505–1510.

Li, W.W., Guo, T.Z., Liang, D.Y., Sun, Y., Kingery, W.S., Clark, J.D., 2012. Substance P signaling controls mast cell activation, degranulation, and nociceptive sensitization in a rat fracture model of complex regional pain syndrome. Anesthesiology 116, 882–895.

Liu, D., Jiang, L.S., Dai, L.Y., 2007. Substance P and its receptors in bone metabolism. Neuropeptides 41, 271–283.

Madsen, J.E., Hukkanen, M., Aune, A.K., Basran, I., Moller, J.F., Polak, J.M., Nordsletten, L., 1998. Fracture healing and callus innervation after peripheral nerve resection in rats. Clin. Orthop. Relat. Res. 230–240.

Marsell, R., Einhorn, T.A., 2011. The biology of fracture healing. Injury 42, 551–555.

Mori, T., Ogata, T., Okumura, H., Shibata, T., Nakamura, Y., Kataoka, K., 1999. Substance P regulates the function of rabbit cultured osteoclast; increase of intracellular free calcium concentration and enhancement of bone resorption. Biochem. Biophys. Res. Commun. 262, 418–422.

Müller, R., Rüegsegger, P., 1997. Micro-tomographic imaging for the nondestructive evaluation of trabecular bone architecture. Stud. Health Technol. Inform. 40, 61–79.

Nilsson, J., von Euler, A.M., Dalsgaard, C.J., 1985. Stimulation of connective tissue cell growth by substance P and substance K. Nature 315, 61–63.

Nishiura, T., Abe, K., 2007. Alpha1-adrenergic receptor stimulation induces the expression of receptor activator of nuclear factor kappaB ligand gene via protein kinase C and extracellular signal-regulated kinase pathways in MC3T3-E1 osteoblast-like cells. Arch. Oral Biol. 52, 778–785.

Nordsletten, L., Madsen, J.E., Almaas, R., Rootwelt, T., Halse, J., Konttinen, Y.T., Hukkanen, M., Santavirta, S., 1994. The neuronal regulation of fracture healing. Effects of sciatic nerve resection in rat tibia. Acta Orthop. Scand. 65, 299–304.

Opolka, A., Straub, R.H., Pasoldt, A., Grifka, J., Grässel, S., 2012. Substance P and norepinephrine modulate murine chondrocyte proliferation and apoptosis. Arthritis Rheum. 64, 729–739.

Sachs, C., Jonsson, G., 1975. Mechanisms of action of 6-hydroxydopamine. Biochem. Pharmacol. 24, 1–8.

Severini, C., Improta, G., Falconieri-Erspamer, G., Salvadori, S., Erspamer, V., 2002. The tachykinin peptide family. Pharmacol. Rev. 54, 285–322.

Sherman, B.E., Chole, R.A., 1995. A mechanism for sympathectomy-induced bone resorption in the middle ear. Otolaryngol. Head Neck Surg. 113, 569–581.

Shih, C., Bernard, G.W., 1997. Neurogenic substance P stimulates osteogenesis in vitro. Peptides 18, 323–326.

Straub, R.H., 2011. Neural regulation of pain and behavior. Firestein-bookElsevier (chapter 29).

Straub, R.H., Wiest, R., Strauch, U.G., Harle, P., Scholmerich, J., 2006. The role of the sympathetic nervous system in intestinal inflammation. Gut 55, 1640–1649.

Takeda, S., Elefteriou, F., Levasseur, R., Liu, X., Zhao, L., Parker, K.L., Armstrong, D., Ducy, P., Karsenty, G., 2002. Leptin regulates bone formation via the sympathetic nervous system. Cell 111, 305–317.

Togari, A., 2002. Adrenergic regulation of bone metabolism: possible involvement of sympathetic innervation of osteoblastic and osteoclastic cells. Microsc. Res. Tech. 58, 77–84.

Wang, L., Zhao, R., Shi, X., Wei, T., Halloran, B.P., Clark, D.J., Jacobs, C.R., Kingery, W.S., 2009. Substance P stimulates bone marrow stromal cell osteogenic activity, osteoclast differentiation, and resorption activity in vitro. Bone 45, 309–320.

Wei, T., Li, W.W., Guo, T.Z., Zhao, R., Wang, L., Clark, D.J., Oaklander, A.L., Schmelz, M., Kingery, W.S., 2009. Post-junctional facilitation of Substance P signaling in a tibia fracture rat model of complex regional pain syndrome type I. Pain 144, 278–286.

Wiens, M., Etminan, M., Gill, S.S., Takkouche, B., 2006. Effects of antihypertensive drug treatments on fracture outcomes: a meta-analysis of observational studies. J. Intern. Med. 260, 350–362.

Wittrant, Y., Theoleyre, S., Couillaud, S., Dunstan, C., Heymann, D., Redini, F., 2003. Regulation of osteoclast protease expression by RANKL. Biochem. Biophys. Res. Commun. 310, 774–778.

Yirmiya, R., Goshen, I., Bajayo, A., Kreisel, T., Feldman, S., Tam, J., Trembovler, V., Csernus, V., Shohami, E., Bab, I., 2006. Depression induces bone loss through stimulation of the sympathetic nervous system. Proc. Natl. Acad. Sci. U. S. A. 103, 16876–16881.

Zimmer, A., Zimmer, A.M., Baffi, J., Usdin, T., Reynolds, K., Konig, M., Palkovits, M., Mezey, E., 1998. Hypoalgesia in mice with a targeted deletion of the tachykinin 1 gene. Proc. Natl. Acad. Sci. U. S. A. 95, 2630–2635.

Please cite this article as: Niedermair, T., et al., Absence of substance P and the sympathetic nervous system impact on bone structure and chondrocyte differentiation in an adult mod..., Matrix Biol. (2014), http://dx.doi.org/10.1016/j.matbio.2014.06.007